CORROSION SCIENCE AND TECHNOLOGY, Vol.10, No.3(2011), pp.87~94

Monitoring of Atmospheric Corrosivity inside Steel Upper Box Girder in Yeongjong Grand Bridge

SeonYeob Li

CorRel Technology, Co., Ltd., 706, I-Dong, Sangnok-Gu, Ansan, Gyeonggi-Do, Korea 426-864
(Received April 13, 2011; Revised June 7, 2011; Accepted June 9, 2011)

The typical corrosion prevention method inside the steel upper box girder in a suspension bridge involves the use of paints. However, in an effort to reduce environmental impact and cost, the suspension portion of the Yeongjong Bridge, Korea utilizes dehumidification systems to control humidity and prevent corrosion inside its box girder. Maintaining a uniform humidity distribution at the proper level inside the box girder is critical to the successful corrosion control. In this study, the humidity and the resultant atmospheric corrosivity inside the box girder of the Yeongjong Bridge was monitored. The corrosion rate of the steel inside the box girder was obtained using thin-film electrical resistance (TFER) corrosion sensors. Time-of-wetness (TOW) measurements and the deposition rates of atmospheric pollutants such as Cl^- and SO_x were also obtained. Classification of the atmospheric corrosivity inside the box girder was evaluated according to ISO 9223. As a result, no corrosion was found in the upper box girder, indicating that the dehumidification system used in the Yeongjong Bridge is an effective corrosion control method.

Keywords *: suspension bridge, Yeongjong Bridge, steel box girder, dehumidification, atmospheric corrosion, corrosivity, thin-film electrical resistance (TFER) sensor*

1. Introduction

The Yeongjong Grand Bridge serves as the gateway to both metropolitan Seoul and the Incheon International Airport (Fig. 1). This two-story bridge is 4,420 m long. A six-lane highway runs along the upper deck while a four-lane highway and a double-track railroad run along the lower deck. Along its span, the bridge utilizes three different types of construction: a self-anchored suspension bridge (550 m), a truss bridge (2,250 m), and a composite Rahmen bridge (1,620 m).

Long-span bridges are generally expected to have a lifetime of at least 100 years, since they have been constructed at an enormous expense and are invaluable elements of social infrastructure.[1] For this reason, the main threats to the reliability of the bridge should be minimized and controlled throughout the whole lifespan of the bridge. One of the threats to the safety of long-span bridges is corrosion. The box girder of a long-span bridge is the superstructure that possesses a larger area in comparison to others. Due to the semi-closed nature of the box girder structure, the penetration of water and salts into the girder is small. Hence, the corrosivity is relatively mild inside the girder compared to the outside, which is exposed directly to the atmosphere. Vassie reported that if water and/or moisture do not penetrate the inside of the box girder, no internal coating of the girder is required.[2] Fujino reported that the corrosion rate of steel inside a box girder is as small as 0.003 to 0.3 μm/y.[3] However, once moisture has penetrated the inside of the girder, dewdrops may form

Fig. 1. The Yeongjong Grand Bridge.

† Corresponding author: syli@correltech.com

on the surface of the steel members depending on the external temperature. These dewdrops result in the development of rust layers. Therefore, the corrosion of the internal surfaces of box girders is typically prevented using painting methods. These methods typically employ non-organic zinc-rich primers and multiple layers of modified epoxy resin paint.

Using paint to prevent corrosion in the box girder is very expensive, both at the time of initial installation and during post-construction periodic maintenance activities. In response to the high cost of painting, a new corrosion protection method involving the control of humidity inside the box girder has been developed and applied throughout the world.[1),4)-7)] This new method prevents rust generation by dehumidifying the air with drying machines. It is generally known that corrosion in an uncontaminated atmosphere does not take place if the relative humidity (RH) in the vicinity of a steel structure is kept below about 60%.[8)] The dehumidification system is more economic than painting. A recent survey claims that the ratio of the life cycle cost (LCC) of the dehumidification system compared to that of the painting system ranged from 0.15 to 0.33.[9)] The dehumidification system is also more environmentally friendly, as it avoids the problems associated with blasting and painting. It was for this reason that dehumidification systems were set up inside the box girder of the suspension portion of the Yeongjong Bridge, which was constructed in 2002.

In this study, the corrosivity of air inside an upper box girder in the self-anchored suspension bridge, located at the center part of the Yeongjong Bridge, was monitored and evaluated using the methods described in ISO 9223.[10)] To prove the effectiveness of the dehumidification system as a corrosion prevention method, the corrosion rate of steel inside the box girder was obtained using thin-film electrical resistance (TFER) corrosion sensors.

2. Experimental procedure

A schematic of the dehumidification system in the Yeongjong Grand Bridge is illustrated in Fig. 2.

The main components of the system are:

- A sorption dehumidification unit with a fresh air intake and moisture laden air discharge
- A fan unit which ensures circulation of the dry air in the box girder.
- Ducting connecting the fan and dehumidification units.
- A pressure equalizing unit which keeps the air pressure inside the box girder approximately equal to the external air pressure.

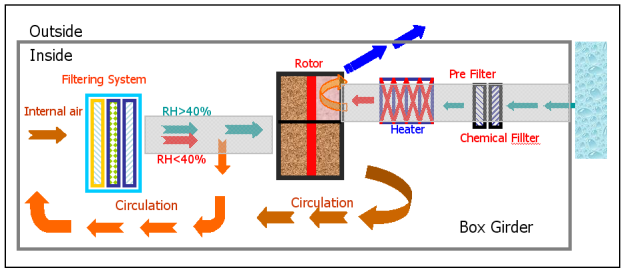

Fig. 2. Principle of Dehumidification System in Yeongjong Bridge.

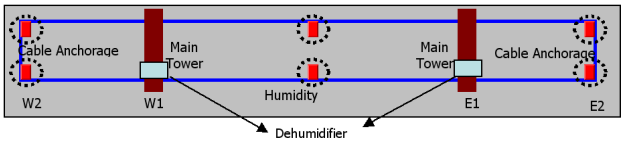

Fig. 3. Location of Six Humidity sensors in Upper Box Girder of Yeongjong Bridge.

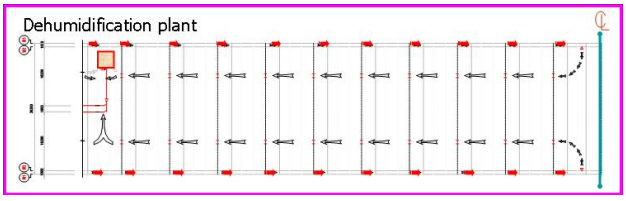

(a)

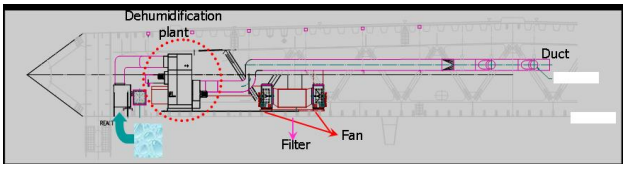

(b)

Fig. 4. Arrangement of Dehumidification System in Yeongjong Bridge, (a) Top View, (b) Cross-sectional View.

The system is generally set to keep the RH at 40%. This allows for sudden changes in temperature and also includes a margin of safety below the maximum level of 60% RH. A total of six humidity sensors are located inside the box girder as shown in Fig. 3. The circulation system is designed for forward air flow through rough stiffeners and fairings and return flow through the box girder as shown in Fig. 4.

Two fundamental approaches to corrosivity classification were applied to evaluate the effectiveness of the dehumidification system in the suspension part of the Yeongjong Bridge. These two methodologies are based on the use of atmospheric parameters and the direct meas-

urement of corrosion rates. When used in a complimentary manner, these two approaches can be used to derive the relationship between the atmospheric corrosion rates and the dominant corrosive parameters. The major benefit of monitoring the atmospheric parameters is that the prediction of corrosivity can be made in a relatively short amount of time, minimizing experimental work. Environmental data was collected inside the upper box girder, and the air temperature and the RH were used to calculate the time-of-wetness (TOW) as described in ISO 9223. This procedure assumes that wetness occurs whenever the RH is equal to or greater than 80% and the temperature exceeds 0 ℃. In addition, so-called "time-of-wetness (TOW)" sensors were also installed to measure the real wetted time of steel surface.[11] Fig. 5 shows the schematic diagram and the photograph of the installed TOW sensor. The surface moisture deposited on the TOW sensor serves as an electrolyte to generate a potential in a moisture-sensing galvanic cell that consists of comb-type alternate electrodes of Cu-Au. The spacing of two electrodes is about 200 μm.

The deposition rates of chloride were assessed using the "dry gauze" method.[12),13)] The following formula was used to compare these deposition rates with the results of the "wet candle" method described in the ISO standard:[12)]

$$Cl_{wet\ \ candle} = 2Cl_{dry\ \ gauze} \quad (1)$$

The deposition rate of sulfur dioxide was determined on alkaline surfaces 110 mm potassium carbonate impregnated cellulose filter (Whatman 1441-110, ashes).[14-15)] The air samplers consisting of dry gauzes and alkaline papers were placed onto the inner wall of box girder as shown in Fig. 6.

Direct measurements of atmospheric corrosivity are generally obtained using special methods such as "Classification of Industrial and Marine Atmosphere (CLIMAT)" devices. These devices are based on a wire-on-bolt test, in which an aluminum wire is wrapped around a copper or steel bolt.[16),17)] Similar test methods have been adopted by ISO, but these tests require a long exposure period. Another measurement approach using a simple corrosion coupon exposure program can also be considerable. However, in a controlled environment where the corrosion rate is relatively small, the additional weight loss could occur during the removal of corrosion products from the coupon in acid solutions. The corrosion rate can therefore be overestimated and unreliable in low corrosivity environments. This is the expected situation inside the upper box girder of the Yeongjong Bridge when the dehumidification system is working well. Therefore, high sensitivity thin-film electrical resistance (TFER) corrosion sensors were used to obtain corrosion rates in this study. The thin films, with a thickness on the order of a micrometer, were deposited by DC magnetron sputtering of carbon steel onto a sintered alumina plate in an Argon atmosphere. The TFER sensors were fabricated using masking and etching in an aqueous 10% $FeCl_3$ aqueous solution. Details of the fabrication and physical characterization of deposited films, including their application in TFER sensors, have been previously reported.[18)-22)] A schematic diagram and a photograph of the fabricated sensor are shown in Fig. 7. The corrosion

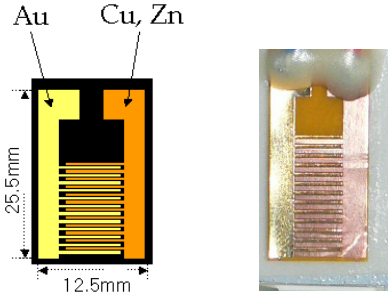

Fig. 5. (a) Schematic diagram, and (b) photograph of TOW sensors (Al-Cu couple).

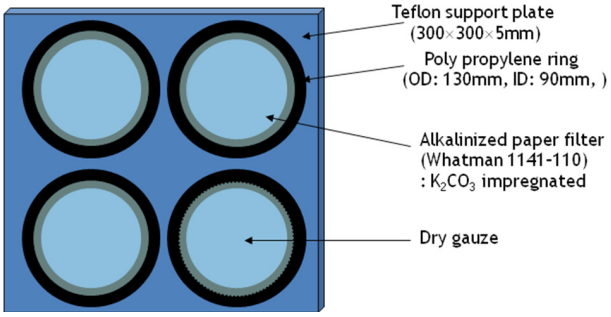

Fig. 6. Schematic Diagram of Pollutants Collection System.

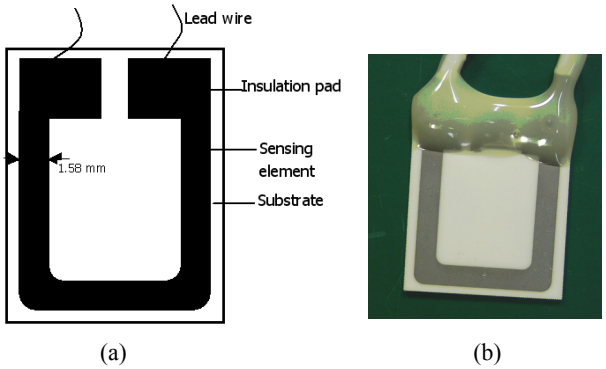

Fig. 7. (a) Schematic Diagram and (b) Photograph of Fabricated TFER Sensor.

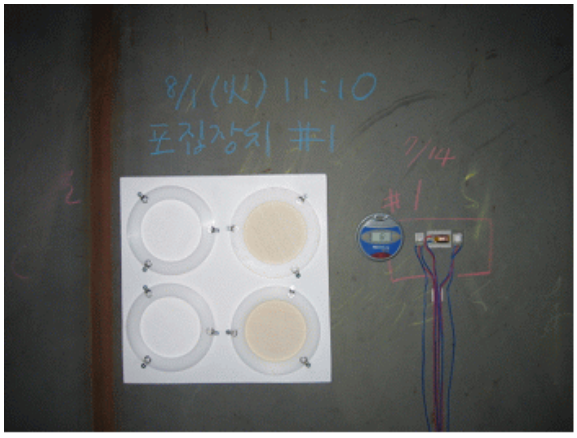

Fig. 8. Installed Sensors and Pollutants Collection System.

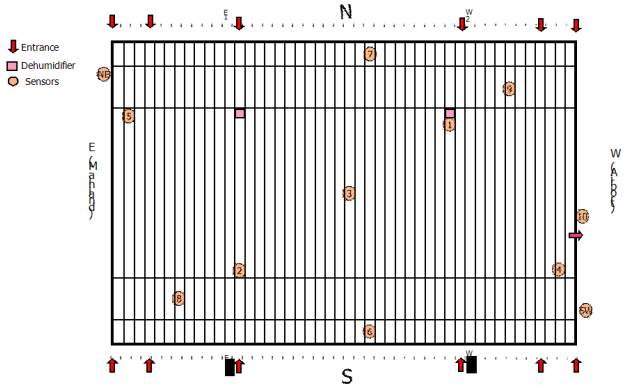

Fig. 9. Locations of Installed Sensors and Pollutants Collection System (Top view).

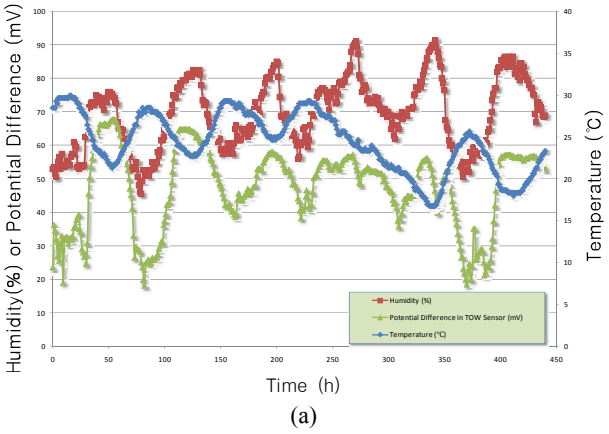

(a)

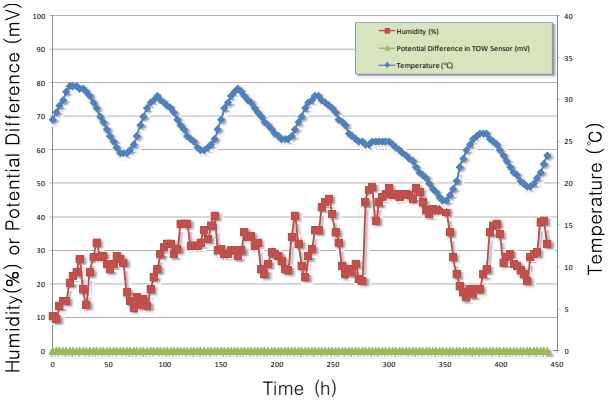

(b)

Fig. 10. Temperature, RH and Potential difference in TOW Sensor Distribution during Summer Season (a) Outside, and (b) Inside Box Girder.

rate of the TFER sensor is proportional to the value of the cross sectional loss of the sensing element. However, for the TFER sensor, it is reasonable to assume that the change in resistance of the sensor is mainly proportional to the change in the thickness, because the plane aspect ratio (width/thickness) is as high as 132. This assumption results in an error in the corrosion rate of about 3%.[20] The remaining thickness was determined by comparing the measured resistance (R) to the initial resistance (R_0). The slope of R_0/R vs. exposure time gave the rate of thickness reduction, i.e., the average corrosion rate. The installed TOW/TFER sensors, pollutants collection system and a digital thermometer/hygrometer are shown in Fig 8.

A total of nine sensors and pollutants collection systems were installed inside the box girder as shown in Fig. 9. The responses of the environmental sensors and the TFER sensors were monitored using data loggers and the pollutant deposition rates were calculated after a six-month exposure.

3. Results and discussion

Fig. 10 shows a typical temperature, RH and the potential differences in the TOW sensor measured inside and outside the box girder during summer season for 450 h. The temperature variation is similar in two cases. However, relatively higher RH values could accelerate the corrosion process in outdoor environment. On the contrary, the RH was kept below about 50% inside the box girder, which could suppress the corrosion process to occur. It is also noticeable that the difference in the response of TOW sensors inside and outside. Outside the box girder, the potential difference in the TOW sensor developed according to the variation of RH, whereas the potential difference inside the box girder was kept zero throughout the entire measurement period, which implies that no moisture was deposited on the sensor surface.

Table 1 shows the environmental data measured inside the box girder over a period of seven months from May through November. Compared to the outdoor environment

Table 1. Environmental Data of Test Locations (Average Values)

Sample No.	Cl^-		SO_2		TOW	
	Deposition rate ($mg/day/m^2$)	ISO categories	Deposition rate ($mg/day/m^2$)	ISO categories	%	ISO categories
1	0.562	S0	0.000	P0	0.06	τ 1
2	0.578	S0	0.000	P0	2.88	τ 2
3	0.622	S0	0.000	P0	2.23	τ 2
4	0.562	S0	0.000	P0	0.00	τ 1
5	0.610	S0	0.000	P0	2.10	τ 2
6 (fairing)	0.650	S0	0.000	P0	2.73	τ 2
7 (fairing)	0.594	S0	0.000	P0	2.00	τ 2
8	0.602	S0	0.000	P0	2.96	τ 2
9	0.594	S0	0.000	P0	0.06	τ 1
10 (outside)	1.220	S0	1.502	P0	47.85	τ 4

Table 2. Corrosion Categories and Expected Corrosion Rates for First Year of Exposure

Sampling point	Corrosivity categories	Corrosion rates, r_{corr}, (mm/y)
1	1	$r_{corr} \leq 0.0013$
2	1	$r_{corr} \leq 0.0013$
3	1	$r_{corr} \leq 0.0013$
4	1	$r_{corr} \leq 0.0013$
5	1	$r_{corr} \leq 0.0013$
6	2	$r_{corr} \leq 0.0013$
7	2	$r_{corr} \leq 0.0013$
8	1	$r_{corr} \leq 0.0013$
9	1	$r_{corr} \leq 0.0013$
10	3	$0.025 < r_{corr} \leq 0.05$

(sample no. 10), the atmospheric environment inside the box girder is significantly less contaminated by chloride and SO_2. In addition, the TOW value (%) inside the girder was low (ISO category T1). The corrosivity categories and expected corrosion rates of carbon steel during the first year of exposure, as determined per ISO standards, are presented in Table 2. It is clear that the environment inside the girder is less corrosive than the outdoor environment. Fig. 11 shows the typical response of the TFER sensor installed (a) inside and (b) outside the box girder. The resistance of the TFER sensor installed inside the box girder was nearly constant, whereas the sensor installed outside showed a gradual increase in resistance, indicating the progress of corrosion. The average corrosion rates obtained from the slope of the response curves are 0.0004 mm/y and 0.03 mm/y, respectively. These measured corro-

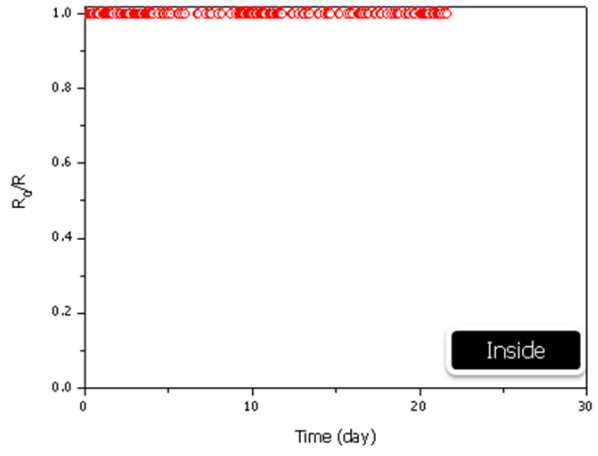

(a)

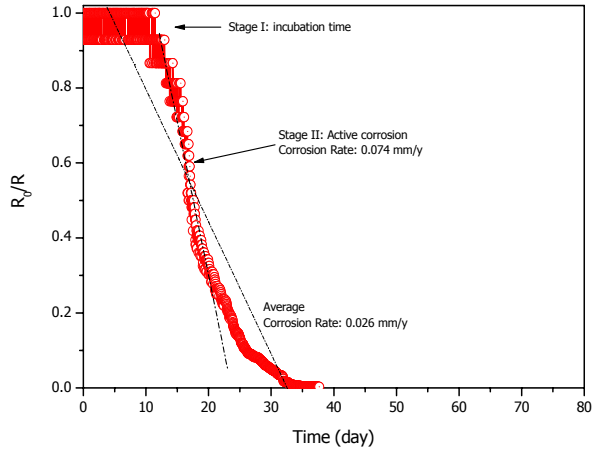

(b)

Fig. 11. Typical Responses of TFER Sensors, (a) Inside box girder, (b) Outside box girder.

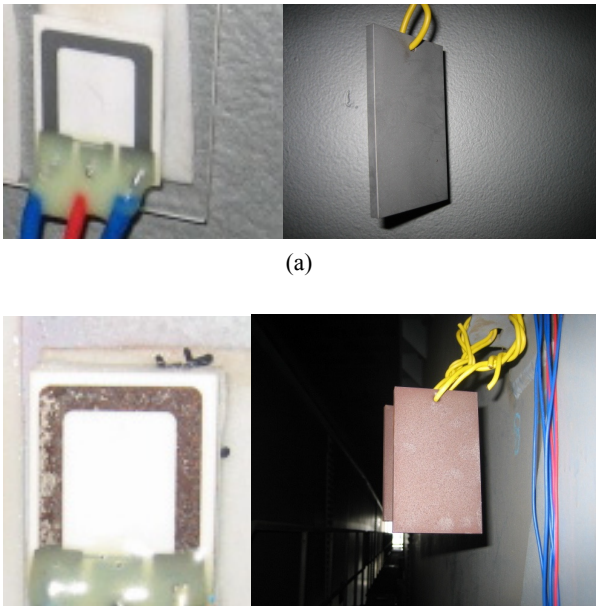

(a)

(b)

Fig. 12. Corrosion Morphologies of TFER Sensors and Coupons, (a) Inside, (b) Outside.

sion rates correlate well with those calculated according to the ISO standard (Table 1). Fig. 12 shows the corrosion morphologies of the sensors and the carbon steel coupons installed together with the sensors. The sensors and coupons installed inside the box girder showed no evidence of corrosion, whereas those installed outside showed the formation of a rust layer.

These results were also confirmed in the laboratory. Testing was performed that simulated the wet/dry cycle and other atmospheric conditions both inside and outside the box girder. Fig. 13 shows the schematics and the experimental set-up of the laboratory tests. Using Table 1 as a guide, synthetic solutions simulating atmospheric components measured inside and outside the box girder were prepared and then sprayed into the test chamber. The wet/dry cycle was controlled using a humidifier and a dryer.[20] The TFER sensors were installed in the test chamber and the response of the sensors was recorded. In addition, a 3.5% NaCl solution was also used for comparison. Fig. 14 shows the response of the TFER sensors during the laboratory experiment. Again, the results are very similar to those of previous measurements, and the differences in the corrosion rates are clear.

The results of all three experiments are summarized in Table 3. The results correlate well with each other, and there is a clear difference in the corrosion rate measured with and without dehumidification. These results confirm that the dehumidification system is a very effective corrosion control method. The corrosion inside the box girder

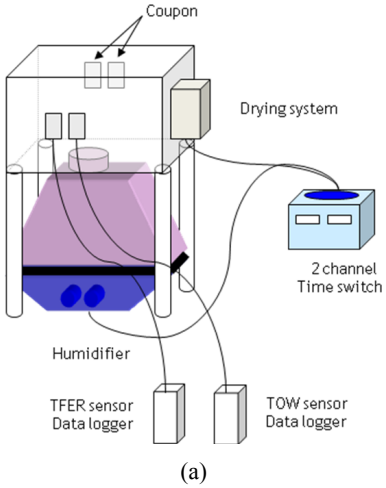

(a)

(b)

Fig. 13. (a) Schematic Diagram and (b) Experimental Set of Laboratory Tests.

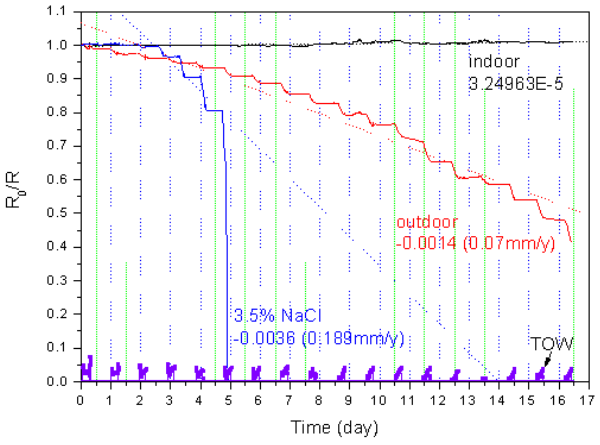

Fig. 14. Responses of TFER Sensors in Laboratory Tests.

is therefore expected to be negligible. Moreover, compared to other indirect methods such as the ISO corrosivity assessment, the direct measurement of the corrosion rates

Table 3. Comparison of Results of Various Experiments

Corrosion Rate (mm/y)	Inside box girder	Outside box girder
ISO methods	< 0.0013	0.025 - 0.05
TFER sensors in field	< 0.0004	~ 0.03
TFER sensors in lab tests	~ 0.0002	0.068

Fig. 15. Corrosion Occurred in Hanger Rope Anchorage Section.

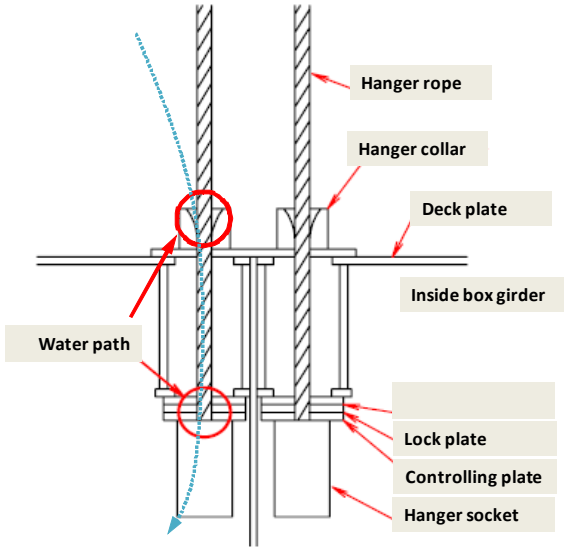

Fig. 16. Schematic Diagram of Water Infiltration Mechanism Through Hanger Rope Anchorage Section.

using TFER sensors yielded quicker and more reliable results.

Even though the performance of the dehumidification system is satisfactory, there is still a possibility of corrosion occurring inside the box girder. Fig. 15 shows an example of corrosion that occurred at the hanger rope anchorage sections of the bridge. In general, the hanger rope is protected from corrosion by a galvanized coating and epoxy painting. The coating materials are typically applied to the inside of the hanger collar, and corrosion protection tape is applied from the deck plate to the lock plate to prevent the ingress of water from the outside (Fig. 16). In spite of these preventative measures, the degradation of the coating materials at the collar parts enabled the penetration of outdoor water through the hanger rope anchorage into the box girder. This example helps illustrate the need for continuous corrosion monitoring of bridges throughout their lifespan. The TFER sensors provide a very promising method for this preventative monitoring.

The Bridge Health Monitoring System (BHMS) is currently installed and operated in the suspension section of the Yeongjong Bridge. Using this system, it is possible to monitor the mechanical integrity of the bridge using a variety of installed sensors, such as accelerometers, seismometers, and strain gauges, etc. As a result of this study, the TFER sensors were additionally installed in the suspension portion of the bridge and incorporated into the BHMS. It is expected that these sensors will aid in early recognition of corrosion problems and extend the service life of the bridge.

4. Conclusion

This paper provides some novel corrosion monitoring method for the upper steel box girder of the Yeongjong Grand Bridge. The following observations and conclusions can be drawn based on the experimental results of this study.

1) With the use of a dehumidification system, the corrosion rate drops to negligible levels inside the upper steel box girder in the Yeongjong Grand Bridge.

2) The results of corrosivity assessment based on the ISO standards and the direct measurement of corrosion rate using the TFER sensors confirms the reliability of the dehumidification systems. In addition, it was found that the TFER sensors are good methods for corrosion monitoring inside the box girder.

Acknowledgments

Financial support of this study from The New Airport Hiway Co., Ltd. and The Corrosion Science Society of Korea is gratefully acknowledged.

References

1. Y. Yanaka and M. Kitakawa, *J. Construct. Steel Res.*, **58**, 131 (2002).

2. P. R. W. Vassie, *British Corros. J*., **22**, 37 (1987).
3. Y. Fujino, *Boushoku Gishutsu*, **38**, 546 (1989).
4. N. J. Gimsing, *Structural Engineering International*, **5**, 210 (1995).
5. K. Masai, M. Yoshiaki, and N. Makoto, *Bridge and Foundation Engineering*, **33**, 31 (1999).
6. K. H. Ostenfeld, *Structural Control and Health Monitoring*, **11**, 125 (2004).
7. O. Sørensen, Box Girders, Design, Fabrication, Operation and Maintenance, *Proceedings of International Orthotropic Bridge Conference*, p. 23, ASCE, Sacramento, CA, August (2004).
8. H. H. Uhlig and R. W. Revie, Corrosion and Corrosion Control, 3rd ed., p.173, John Wiley & Sons, Inc., New York, NY (1985).
9. J. Liao, S. Matsui, T. Shinohara, and Y.Fujino, *Kurimoto Technical Bulletin*, **52**, 2 (2005).
10. ISO 9223, Corrosion of metals and alloys - Corrosivity of atmospheres - Classification, International Standards Organization (ISO), Geneva, Switzerland (1992).
11. ASTM G84, Standard Practice for Measurement of Time-of-Wetness on Surfaces Exposed to Wetting Conditions as in Atmospheric Corrosion Testing, ASTM International, West Conshohocken, PA (1993).
12. JIS Z2382, Determination of pollution for evaluation of corrosivity of atmospheres, Japanese Industrial Standards Committee, Tokyo, Japan (1998).
13. P. V. Strekalov and Y. M. Panchenko, *Zachita Metallov*, **28**, 269 (1992).
14. ISO 9225. Corrosion of metals and alloys - Corrosivity of atmospheres - Measurement of pollution, International Standards Organization (ISO), Geneva, Switzerland (1992).
15. V. Etymezian, C. I. Davidson, S. Figner, M. F. Striegel, N. Barabas, and J. C. Chow, *JAIC*, **37**, 187 (1998).
16. ASTM G116, Standard Practice for Conducting Wire-on-Bolt Test for Atmospheric Galvanic Corrosion, ASTM International, West Conshohocken, PA (1993).
17. D. P. Doyle and T. E. Wright, Rapid Methods for Determining Atmospheric Corrosivity and Corrosion Resistance, *Atmospheric Corrosion*, W.H. Ailor, ed., John Wiley & Sons, Inc., New York, NY (1982).
18. S. W. Jung, S. Y. Li, and Y. G. Kim, *Electrochem. Commun*., **8**, 658 (2006).
19. Y. G. Kim, S. Y. Li, S. W. Jung, S. M. Lee, J. Kim, and Y. T. Kho, *Surf. Coat. Technol*., **201**, 1931 (2006).
20. S. M. Lee, S. Y. Li, S. W. Jung, Y. G. Kim, H. S. Song, and D. S. Won, *Corro. Sci. Tech.*, **5**, 112 (2006).
21. S. Y. Li, Y. G. Kim, S. W. Jung, H. S. Song, and S. M. Lee, *Sens. Actuators B: Chem*., **120**, 368 (2007).
22. S. Y. Li, S. W. Jung, K. W. Park, S. M. Lee, and Y. G. Kim, *Mater. Chem. Phys*., **103**, 9 (2007).